Journal of Building Engineering 33 (2021) 101580

Contents lists available at ScienceDirect

Journal of Building Engineering

journal homepage: http://www.elsevier.com/locate/jobe

Hybrid cooling system integrating PCM-desiccant dehumidification and personal evaporative cooling for hot and humid climates

Mohamad El Loubani [a], Nesreen Ghaddar [a,*], Kamel Ghali [a], Mariam Itani [a,b]

[a] Mechanical Engineering Department, American University of Beirut, P.O. Box 11-0236, Beirut, 1107-2020, Lebanon
[b] Mechanical Engineering Department, Phoenicia University, District of Zahrani, Lebanon

ARTICLE INFO

Keywords:
Phase change material
Solid desiccant wheel
Trombe wall
Personalized evaporative cooling

ABSTRACT

Hot and humid climates present a challenge for implementing passive cooling practices in office spaces, due to the inherent small temperature difference between day and night, which affects the utilization of thermal storage systems. Moreover, added means are required to maintain the humidity in the space at an acceptable level for comfort. The novelty of this study is to design and implement a feasible hybrid cooling system for office spaces in such climates by uniquely combining several sustainable cooling, thermal storage, and dehumidification solutions. The proposed system integrates a phase change material (PCM) thermal storage layer with a melting temperature of 25 °C to cool the supply air and a personalized evaporative cooler (PEC) to provide cooling for the occupants. The supply air humidity is controlled using a solid desiccant wheel regenerated via an auxiliary heater assisted with a Trombe wall. Mathematical models were adopted for each system component/process, solved numerically and integrated to size the system components, simulate their operation and predict the overall system's performance in an office space during the summer months of Beirut climate. The proposed system was found to achieve acceptable thermal comfort levels in the space. Moreover, it reduced the total energy cost by 87% compared with a conventional air conditioning unit over the summer period. In addition, the Trombe wall provided energy savings of 55% compared to relying only on the auxiliary heater. Hence, integrating several sustainable solutions succeeded in implementing an effective cooling system of office spaces in hot humid climates.

1. Introduction

Conventional heating, ventilation, and air conditioning (HVAC) systems are widely used for cooling or heating purposes, thermal comfort provision, and indoor air quality improvement in buildings [1]. However, these systems consume a large amount of energy amounting to nearly 40% of the total building energy consumption [2]. In addition, they negatively impact the environment accounting for more than 30% of carbon dioxide emissions [2]. They also disrupt the energy supply and demand balance in hot and humid climates [3]. Therefore, sustainable and passive alternative techniques are primarily sought to reduce the use of conventional HVAC systems [4]. One of the passive cooling techniques is the free cooling of buildings [5]. Free cooling ventilation uses the outdoor air as a heat sink for building cooling purposes [6,7]. Conventional free cooling can be implemented in moderate climates when the outdoor air temperature is within the thermal comfort range of temperatures. However, in hot climates the outdoor air temperature is higher than the thermal comfort level. Therefore, to benefit from free cooling in these climates, the natural cold energy at night due to outdoor air temperature difference between day and the night, should be utilized [8]. As a result, a storage system is typically added to collect this energy for use during the warm period of the following day. A sustainable passive storage system that can be used for this purpose is known as thermal energy storage [9,10]. However, hot and humid climates present a challenge in utilizing free cooling even with the implementation of thermal storage. Hot and humid climates, unlike arid or semi-arid climates, are characterized by a small temperature difference between day and night, which affects the selection and performance of thermal storage systems and results in elevated space temperature that may not provide the desired level of thermal comfort [11]. However, the elevated space temperature issue can be resolved with the use of a personalized cooling system that provides cooling to the upper human body and hence ensures comfort at high background space temperature [12]. Even so, the requirement for the humidity in the space to be maintained at an acceptable level for comfort purposes means that fresh air supply must

* Corresponding author.
E-mail address: farah@aub.edu.lb (N. Ghaddar).

https://doi.org/10.1016/j.jobe.2020.101580
Received 15 March 2020; Received in revised form 11 June 2020; Accepted 12 June 2020
Available online 17 June 2020

Nomenclature

A	area, m^2
C_p	specific heat, J/kg·K
COP	coefficient of performance
f	melting fraction
h	convective heat transfer coefficient, $W/m^2 \cdot K$
H	enthalpy, J/kg
h_{fg}	latent heat of vaporization of water, J/kg
h_{sf}	latent heat of fusion of the PCM, J/kg
I	solar radiation, W/m^2
k	thermal conductivity, W/m·K
L	length of the PCM layer, m
$\dot{m}$	mass flow rate, kg/s
PF	performance factor
Q	power, W
T	temperature, °C
t	time, s
t_e	thickness of envelope component, m
U	overall heat transfer coefficient, $W/m^2 \cdot K$
V	volume, m^3
w	humidity ratio, kg/kg
Greek symbols	
α	absorptivity
ε	emissivity
μ	efficiency (%)
ρ	density, kg/m^3
τ	transmissivity
$\varnothing$	relative humidity, %
Subscripts	
amb	ambient air
aux	auxiliary heater
ch	air channel
cond	conduction through the wall
conv	convection between the room air and walls
EC	air leaving evaporative cooler
eq	equipment sensible load
g	glazing
occ	occupants sensible load
out	dehumidified air leaving desiccant wheel
PEC	personalized evaporative cooler
pcm	phase change material
pcm,melting	phase change material melting phase
r	room air
rad	radiation
reg	regeneration air
sup	supply air
W	wall
wb	ambient wet bulb temperature

be treated to reduce its humidity in the space [13]. While many studies researched and reported feasible passive cooling systems for non-humid climates, there are very few that consider the design of passive cooling systems including associated cooling thermal energy storage that can be applied in hot and humid climates. It is of interest to consider a number of sustainable passive cooling solutions that can cooperate to overcome the above-mentioned challenges in hot and humid climates.

Thermal energy storage is a passive technique that can preserve energy when it is extracted as needed [1]. One of the thriving techniques to store thermal energy is the implementation of phase change materials (PCMs) [9,14]. PCMs are characterized by their ability to store and release large amounts of energy nearly isothermally [10,15]. PCM can be installed into a building in passive systems through integrating them into the building envelope (walls, roofs, and floors) [16–19]. Integrating PCM in building envelopes can enhance the energy storage capacity [18], reduce energy consumption, and improve thermal comfort of the occupants [20]. It was discovered that PCM integrated in buildings is effective in climates where the temperature difference between day and night is large [8]. Osterman et al. [21] conducted an experiment of integrating PCM in a building in Slovenia and their findings were that the maximum cooling potential was in August and July when there were more fluctuations in temperature between day and night. However, there are many humid climates where the temperature difference between day and night is small such as the Mediterranean coastal areas including the Lebanese coast. Therefore, to be able to benefit from thermal energy storage systems, techniques of cooling the outdoor air are required such as evaporative cooling coupled with selecting PCMs at a moderate melting temperature. However, selecting a PCM with a moderate melting temperature may not be low enough to provide room air temperature within thermal comfort levels. Consequently, another passive strategy should be combined with the PCM to assist in cooling the occupied space.

A promising passive personal cooling system that can assist the PCM in providing thermal comfort is the personalized evaporative cooler (PEC). The concept of personalized ventilation relies on transporting and delivering the conditioned air directly to the occupant's face and chest [12,22]. Zhang [11] showed that upper body parts have a dominant impact on the overall sensation while cooling. Thus, the overall thermal comfort of the occupant was improved without the need for having homogenous cool air in the occupant's whole-body microclimate. This permitted the use of elevated supply air temperatures to the space resulting in higher background or macroclimate room temperature [23–25]. Consequently, the PEC would be attractive to use in passive applications where the background room air temperature is at the high end. The PEC can cool the area around the person while only consuming a small amount of water and electrical energy for operating the fan. Cooling is done by water evaporation, which can reduce the temperature of the air when the air is relatively dry [26]. However, a dehumidification strategy is needed to maintain the room air at acceptable humidity such that the PEC can be employed in humid climates of coastal regions.

For this purpose, desiccant dehumidification presents an attractive option in these applications when outside air is humid [27]. There are mainly two types of desiccant dehumidification: solid and liquid desiccants. Liquid desiccants are often integrated with a sustainable energy source such as the one used by Seblani et al. [28]. However, the drawback of the liquid desiccant is that it is carried over by the air stream during the dehumidification and regeneration processes [29]. Although solid desiccants cause a pressure drop while passing through the desiccant material [29], it will not pose an issue for an application that uses fans to circulate the air. Solid desiccant wheels are widely employed as a dehumidification system and can be regenerated using a low-grade regeneration heat source [27]. The heat source could be a free source of heat such as solar energy as implemented by Rambhad et al. [30] who investigated the feasibility of regenerating a solid desiccant wheel using a parabolic trough solar collector. Regeneration could also be achieved by using an electric heater as used by Jani et al. [31] as part of their hybrid space cooling system. In addition, desiccant regeneration can be attained by using a hybrid heat source such as the one used by Heidari et al. [16], which uses a solar assisted boiler for regeneration.

Since passive strategies are sought, regeneration using the building façade as a solar air heater is considered. Mei et al. [32] have used this strategy such that the abundant solar energy available during the summer is utilized to drive an adsorption cooling system. Since the solar energy varies throughout the day, auxiliary heating is needed along with the Trombe wall to reach the necessary desiccant regeneration temperature for maintaining indoor air quality.

In this study, a hybrid cooling system is proposed combining a PCM storage layer, a PEC, and a solid desiccant wheel regenerated via an auxiliary heater aided with a Trombe wall. This system can be carried out in hot and humid regions such as the Mediterranean or the Gulf coastal regions. The proposed system is applicable for unoccupied office spaces during the night to allow for thermal energy storage by the PCM. The proposed system supplies a minimum amount of fresh air according to ASHRAE standards (7 l/s per person) [33] and provides thermal comfort with minimal electric energy divided between the energy of operating small fans and an auxiliary heater. Moreover, the proposed system consumes a minimal amount of water for operating the evaporative cooler and the PEC. Mathematical models of each component are developed to predict the performance of the overall integrated system. The thermal comfort and the overall energy consumption of the system are assessed and are compared with the conventional HVAC system.

The contribution of this work hinges on designing a sustainable hybrid cooling system that can be used for hot and humid climates. The use of a PCM thermal storage system with a moderate melting temperature along with the use of evaporative cooling to cool the ambient air at night, resolves the challenge of free cooling for humid climates, which typically have a small outdoor temperature difference between day and night. However, personalized evaporative cooling, which consumes minimal energy, is proposed to provide thermal comfort to the occupants. The outdoor air is humid and therefore cannot be used to refresh the room air, which in turn has become humid due to of the latent load of the occupants and the use of personal evaporative cooling. Hence, a passive dehumidification strategy to maintain the room relative humidity at acceptable levels is adopted. Using solid desiccant wheels comes with the challenges of mainly finding a passive regeneration technique. For this purpose, the building's façade is suggested as a regeneration source through integrating a Trombe wall at the south façade of the building space. Therefore, the novelty of this study is in integrating several systems and components to deliver a sustainable hybrid cooling system that can be useful for hot and humid climates.

2. System description

The proposed system has two modes of operation: daytime and nighttime operation as shown in Fig. 1 (a) and (b). The system is composed of two main subsystems:

1) Dehumidification system with its regeneration made up of i) desiccant wheel, ii) Trombe wall, and iii) auxiliary heater.
2) Hybrid cooling system made up of i) sensible wheel, ii) evaporative cooler, iii) PCM storage layer system, and iv) PEC.

The proposed operation of the integrated system is studied during daytime and nighttime.

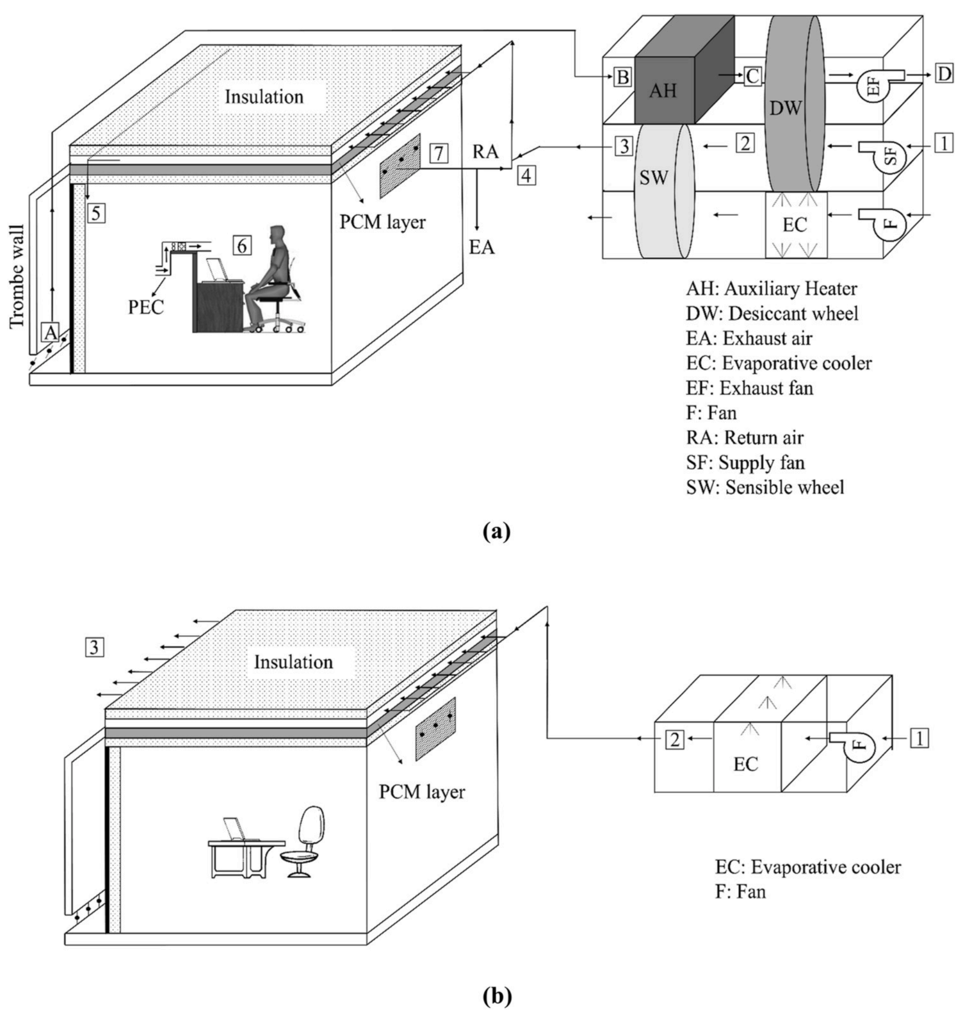

Fig. 1. Schematic of the proposed system during (a) daytime and (b) nighttime operation.

2.1. Daytime operation

Outdoor air at (1) is dehumidified after passing through the desiccant wheel to reach (2). The air gains heat after the dehumidification process so to pre-cool the air, an evaporative cooler is used due to its simplicity and easy implementation to cool a stream of ambient air that can in turn sensibly cool the dehumidified air as it passes through the sensible wheel to reach (3). The evaporatively cooled ambient air leaves the sensible wheel and is exhausted without entering the space. The needed fresh air mixes with the room return air that will recirculate in the space at (4). After cooling the mixed air stream through exchanging heat with the PCM storage layer, the air is supplied to the space at (5). The PEC then draws the room air and supplies the face and the trunk of the occupant with the evaporatively cooled air at (6). Finally, part of the room air is exhausted to the ambient while the other part at (7) is mixed with the fresh outdoor air with the process repeating itself throughout the day. As for the regeneration of the desiccant wheel, firstly, the Trombe wall heats the outdoor air at (A) to reach (B) then the air passes through the auxiliary heater at (C), which will heat the air to the desired regeneration temperature. As the air leaves the auxiliary heater, the air passes through the desiccant wheel to regenerate it and the air exiting the wheel at (D) is then exhausted into the ambient.

2.2. Nighttime operation

The operation of the system during nighttime is shown in Fig. 1(b). A control strategy is implemented to supply fresh outdoor air 3 h before the start of the occupancy schedule. This will refresh the room air with the cooler and less humid outdoor air available during the early hours of the morning. As for the remaining unoccupied hours, a small flow of outdoor air enters the space due to infiltration. The nighttime operation is also used to solidify the PCM from the cool energy available at night. A control strategy is implemented to optimize the solidification process when the ambient air is only admitted to the PCM air channel if its dry bulb temperature is less by 1.5 °C or more than that of the PCM melting temperature. Otherwise, evaporative cooling is used to aid the solidification process of the PCM during the unoccupied hours. Evaporative cooling at best can reduce the ambient air temperature to its wet bulb value; thus, if the temperature of the air leaving the evaporative cooler is below the PCM melting temperature, the outdoor air is drawn to the evaporative cooler, which it cools from (1) to (2). The air then cools the PCM layer and leaves with a higher temperature at (3). When complete solidification is achieved and the PCM temperature at the end of the channel is 1 °C less than the PCM melting temperature, both the evaporative cooler and the fan used to circulate the air will not be used, and no ambient air is introduced to the PCM air channel.

3. Materials and methods

The materials and methods used in this study involve conducting simulations to assess the performance of the proposed hybrid cooling system. Mathematical models corresponding to each subsystem were adopted from published validated literature models for the: i) space model [34,35], ii) PCM system model [17], iii) PEC and thermal comfort model [36], and iv) desiccant dehumidification model [37,38] with its regeneration system that uses a Trombe wall [39,40] and an auxiliary heater. The models were integrated to find the conditions of the supply air, the room air, and the air reaching the occupant. In addition, the thermal comfort of the occupants was assessed using a segmental bio-heat model and a comfort model suitable for non-uniform environments around the occupant. The mathematical models of the subsystem are described in the following sections along with the methodology for sizing the system components.

3.1. Space model

Assuming that the room air is homogeneous and that well mixed conditions apply, the lumped energy and mass balance equations for the office space can be presented as

$$\rho_{air} V_r C_p \frac{dT_r}{dt} = \dot{m}_{sup} C_p \left(T_{sup} - T_r\right) + Q_{occ} + Q_{eq} + Q_{conv} \tag{1}$$

$$\rho_{air} V_r \frac{dw_r}{dt} = \frac{Q_{latent}}{h_{fg}} - \dot{m}_{sup} \left(w_r - w_{sup}\right) - \dot{m}_{PEC} \left(w_r - w_{PEC}\right) \tag{2}$$

where the left side of Eq. (1) represents the transient heat stored in the room air and the first term of the right side is the net convective heat flow. ρ_{air} is the air density (kg/m3), V_r is the volume of the room (m3), C_p is the specific heat capacity of air (J/kg·K), $\dot{m}_{sup}$ is the flow rate of the air supplied to the space (kg/s), T_r and T_{sup} are the room and supply temperature, respectively (°C), Q_{occ} and Q_{eq} are the sensible loads generated by the occupants and electrical equipment in the space including lights, respectively (W), and Q_{conv} is the convective heat transfer between the room air and the envelope of the space (W).

The left side of Eq. (2) represents the transient moisture contained in the room air. The first term of the right side is the moisture generation rate in the room, the second term of the right side corresponds to the net convective moisture flow, and the last term of the right side represents the moisture flow from the air leaving the PEC nozzle to the room air. w_r, w_{sup}, and w_{PEC} are the room supply and air leaving PEC humidity ratios, respectively (kg/kg). Q_{latent} is the latent load generated by the occupants (W), h_{fg} is the latent heat of vaporization of water (J/kg), and $\dot{m}_{PEC}$ is the flow rate of the air supplied by the PEC (kg/s).

The walls' surface and internal temperatures were found using the space model presented by Yassine et al. [34] and Hourani et al. [35] where 1D transient conduction is assumed and each wall is divided into parallel layers. The temperature across these layers is measured while taking into account the ambient and indoor conditions of the boundary layers of each wall.

3.2. PCM system model

The schematic of the PCM storage layer system is shown in Fig. 2. This system is composed of a single PCM layer and a parallel single air channel above it, both sandwiched between insulation layers.

The model of Lin et al. [17] was adopted in this study, which was experimentally validated. The assumptions used to model this system include negligible conduction between two adjacent PCM bricks due to the high contact resistance between the bricks. In addition, the ceiling was assumed to be well-insulated so there was no heat transfer between the PCM and the ceiling. The model used the enthalpy method to simulate the PCM performance while assuming 1-D transient heat transfer. Moreover, the PCM layer consisted of PCM bricks and the air channel was divided into elements of dimensions equal to that of the PCM brick so that each element has a uniform temperature (see Fig. 2).

The energy balance equation at any time t for each element i of the

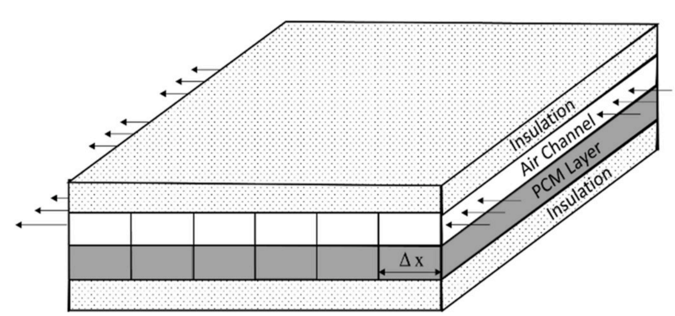

Fig. 2. Schematic of the PCM storage system.

air channel is as follows:

$$\rho_{air} V_i C_p \frac{dT_{air,i}}{dt} = h_{air-pcm} A_i (T_{PCM,i} - T_{air,i}) + \dot{m}_{sup} C_p (T_{air,i-1} - T_{air,i}) \tag{3}$$

where the left side represents the transient heat storage in the air channel. The first term of the right side constitutes the convective heat transfer between the PCM and the air layer and the last term of the right side corresponds to the net convective heat flow. V_i is the volume of a single element (m^3), $h_{air\text{-}pcm}$ is the convective heat transfer coefficient between the air channel and PCM layer ($W/m^2 \cdot K$), A_i is the area of a single element (m^2), $T_{air,i}$ and $T_{PCM,i}$ are the temperatures of the considered air and PCM elements, respectively (°C), and $T_{air,i\text{-}1}$ is the temperature of the element just before the considered element (°C).

As for the PCM layer, the heat exchange is defined for two modes: 1) sensible heat exchange and 2) phase change heat exchange. In the sensible heat exchange, the PCM layer exchanges sensible heat with the air without any occurring PCM phase change and during in which the PCM temperature is different than its melting temperature. The energy balance equation that was used to solve for the PCM temperature is the following:

$$\rho_{pcm} V_i C_{p-pcm} \frac{dT_{pcm,i}}{dt} = h_{air-pcm} A_i (T_{air,i} - T_{PCM,i}) \tag{4}$$

where the left side of the equation represents the transient heat storage in the PCM layer and the right side is the convective heat transfer between the PCM and air layer. ρ_{pcm} is the density of the PCM (kg/m^3) and $C_{p\text{-}pcm}$ is the specific heat of the PCM ($J/kg \cdot K$).

In the phase change heat exchange where the PCM temperature is equal to its melting temperature, the PCM undergoes an isothermal heat exchange until it completely solidifies or completely liquefies. In this case, the melting fraction of the PCM element can be found using the following energy balance equation:

$$\rho_{pcm} V_i h_{sf} \frac{df_i}{dt} = h_{air-pcm} A_i \left(T_{air,i} - T_{PCM,melting}\right) \tag{5}$$

The left side of the equation represents the transient heat storage in the PCM layer while the right side of the equation corresponds to the convective heat transfer between the PCM and air layer. h_{sf} is the latent heat of fusion of the PCM (J/kg), f is the melting fraction of the PCM in element, and $T_{PCM,melting}$ is the melting temperature of the PCM (°C).

Solidification of the PCM during unoccupied hours is achieved through either admitting ambient air directly into the air channel or admitting the evaporatively cooled ambient air. The following equations represent the control strategy implemented to solidify the PCM:

$$\begin{cases} \text{if } T_{amb} \leq T_{PCM,\ melting} - 1.5^{\circ}C \quad \text{then} \quad \text{Evaporative cooler OFF} \\ \text{else} \qquad\qquad\qquad\qquad\qquad\qquad \text{Evaporative cooler ON} \end{cases} \tag{6}$$

The direct single stage evaporative cooler used and the model implemented to predict the temperature of the air leaving the evaporative cooler were the same ones adopted by Hourani et al. [35] and are represented by the following equation:

$$T_{EC} = T_{amb} - PF(T_{amb} - T_{wb}) \tag{7}$$

where T_{EC} is the temperature of the air leaving the evaporative cooler. PF is the performance factor of the evaporative cooler, which could also be considered for its effectiveness and which has a typical value in the range between 80 and 90% as reported by Hourani et al. [35] and experimented by Refaie et al. [41]. Therefore, so an average efficiency of 85% was used.

Once the temperature of the last PCM element is below its melting temperature by 1 °C then the PCM is completely solidified and the evaporative cooler and the fan used to circulate the air are turned off.

3.3. PEC and thermal comfort model

The PEC extracts air from the room using a small fan and cools the air after passing it over a wet pad. This increases the moisture content of the air while decreasing its temperature. The PEC affects only the climate within the vicinity of the occupants, consequently affecting their head and the trunk. Although the PEC creates a relatively higher humidity microclimate around the occupant, humans can tolerate large variations in humidity compared to temperatures [26]. To calculate the thermal comfort of the occupants in non-uniform environmental conditions, Zhang et al. [36] developed a model capable of predicting the overall thermal comfort level using the segmental skin and core temperatures. To measure the skin and core temperatures, Salloum et al. [42] developed a bioheat model capable of predicting the segmental temperature of 11 body segments (head, chest, back, abdomen, buttocks, upper arm, lower arm, hands, thighs, calves, and feet). Once the segmental temperatures are determined, the level of thermal comfort can be calculated and is reflected by the scale developed by Zhang et al. [36], ranging from −4 (very uncomfortable) to +4 (very comfortable).

The different types of evaporative cooling pads including corrugated paper, aspen fiber, and rigid cellulose have a high average performance factor of 90% as studied by Kulkarni et al. [43]. To estimate the temperature of the air leaving the PEC nozzle, the same model for the evaporative cooler can be used.

3.4. Desiccant wheel model

The type of desiccant used in this study is Silica gel due to its high absorption capacity, which can go up to 40% of its weight [37]. Moreover, its adsorption characteristics over a wide range of humidity make it the first choice for solid desiccants [37]. The psychometric model developed and experimentally validated by Beccali et al. [37] and used by Hourani et al. [35] was employed to predict the performance of the solid desiccant wheel of the proposed system. The model was reported to be valid if the supply and regeneration air were in a counter flow arrangement with equal flow rates [38].

The said model predicts the conditions of the dehumidified air (enthalpy and relative humidity) given the conditions of the outdoor and the regeneration air with the equations shown below:

$$H_{out} = 0.1312\, H_{reg} + 0.8688\, H_{amb} \tag{8}$$

$$\varnothing_{out} = 0.9428\, \varnothing_{reg} + 0.0572\, \varnothing_{amb} \tag{9}$$

where H_{out}, H_{reg}, and H_{amb} are the enthalpies of the dehumidified air leaving the desiccant wheel, the regeneration air, and the ambient air (J/kg), respectively whereas φ_{out}, φ_{reg}, and φ_{amb} are the relative humidity of the dehumidified air leaving the desiccant wheel, the regeneration air and the ambient air (%), respectively.

The model correlations were reported to be valid for inlet temperatures between 20 °C and 34 °C, regeneration temperatures between 40 °C and 80 °C, inlet air humidity ratios between 8 and 15 g/kg, and regeneration air humidity ratios between 10 and 16 g/kg [37].

3.5. Regeneration of the desiccant wheel

A heat source is required to regenerate the desiccant wheel. This heat source can be obtained from the free energy provided by the sun during the day. Thus, the use of the Trombe wall to heat the air for regenerating the desiccant wheel proved useful as a passive sustainable strategy. The Trombe wall heats the ambient air flowing through the channel between the wall and the glazing where the heated air passes through the desiccant wheel for regeneration. A similar configuration of the Trombe wall as Badawiyeh et al. [39] and Ong et al.'s [40] was employed in this study such that 1D quasi-steady heat transfer through the Trombe wall was assumed while considering uniform temperatures within each of the glazing and the air channel. The flow rate passing through the air channel of the Trombe wall was set equal to the flow rate of the fresh air passing through the desiccant wheel. The model takes the ambient weather data, glazing properties, wall properties, dimensions of the air channel, and the airflow passing through it as input (more details can be found in section 5). The outputs of the model are the temperatures of the glazing and air channel (uniform temperatures), and the external boundary of the wall.

The energy balance equations of the glazing, air channel, and wall are used to obtain the outputs of the model and are shown below:

$$\alpha_g I + h_{rad}(T_W - T_g) + h_{ch-g}(T_{ch} - T_g) = h_{amb}(T_g - T_{amb}) + Q_{rad-amb} \tag{10}$$

$$h_{ch-W}(T_W - T_{ch}) = h_{ch-g}(T_{ch} - T_g) + \frac{\dot{m}_{ch} C_p (T_{ch} - T_{amb})}{A_{ch}} \tag{11}$$

$$\tau \alpha_W I = h_{ch-W}(T_W - T_{ch}) + h_{rad}(T_W - T_g) + Q_{cond} \tag{12}$$

where the first, second and last terms of the left side of Eq. (10) represent the absorbed solar radiation by the glazing, the radiation between the wall and the glazing, and the convection between the air flowing through the channel with the glazing, respectively. The first term of the right side corresponds to the convection between the ambient air and the glazing and the radiation between the glazing and the ambient whereas the last term of the right side of Eq. (11) represents the flow of air through the channel. The first term of the left side of Eq. (12) is the portion of solar radiation transmitted through the glazing and absorbed by the wall.

α_g is the absorptivity of the glazing, I is the solar radiation (W/m^2), h_{rad} is the radiation heat transfer coefficient between the wall and the glazing (W/m^2·K), $h_{ch\text{-}g}$ and $h_{ch\text{-}W}$ are the convective heat transfer coefficients between the air in the channel and the glazing and between the air in the channel and the wall, respectively (W/m^2·K). T_g, T_{ch}, and T_W are the temperatures of the glazing, air in the channel and wall, respectively (°C). h_{amb} is the convective heat transfer coefficient between the glazing and ambient air (W/m^2·K), $Q_{rad\text{-}amb}$ is the radiation heat transferred between the glazing and ambient air (W), $\dot{m}_{ch}$ is the flow rate of the air passing through the channel (kg/s), A_{ch} is the area of the channel (m^2), τ is the transmissivity of the glazing, α_W is the absorptivity of the wall, and Q_{cond} is the heat conducted through the wall (W).

A schematic of the Trombe wall along with the parameters used are illustrated in Fig. 3.

The air leaving the channel of the Trombe wall at an elevated temperature (T_{ch}) is used to regenerate the desiccant wheel. If the Trombe wall was not enough to heat the air to the required regeneration temperature, other means of heating were implemented such as auxiliary heating.

3.6. Numerical methodology

The sequence of the proposed system's operation is summarized by the flow chart shown in Fig. 4. Firstly, the input parameters of the system were first defined at each hour of operation. Secondly, the desiccant wheel model was implemented to find the characteristics of the dehumidified air using the ambient conditions along with the regeneration conditions. The PCM model was then used to find the supply temperature using Eq. (3) which represented 1D transient heat transfer between the PCM layer and the air channel. The PCM layer was made up of PCM bricks that were 10 cm long and the air channel was discretized accordingly into elements of equal length of 10 cm. Fig. 5(a) shows the discretization method implemented where n is the total number of PCM bricks, L is the total length of the PCM, and Δx is the length of 1 individual PCM brick (10 cm). The space model was used to calculate the room macroclimate air temperature and humidity using Eq. (1) and Eq. (2) where each envelope component (walls, ceiling, and floor) was discretized into N finite volume elements along the thickness of the envelope component (t_e) each having a size Δx that is 0.6 cm thick as shown in Fig. 5(b). Finally, the PEC model was used to calculate the temperature of the air reaching the occupant's upper body parts so that the thermal comfort model was used to assess the thermal comfort of the occupants. The equations were solved using the finite volume method and an implicit scheme was implemented. The implicit scheme allowed for a larger time step to be adopted so that a time step of 360s reduced the simulation runtime. The PCM, space, and PEC models were coupled so that the output parameters were initialized and were obtained by iterations until convergence was reached with an error less than 10^{-4}. After convergence was attained, the model moved to the next time step until the simulation time ended. The simulation was performed for several days to eliminate the effect of initialization on the performance of the system and to obtain a steady periodic solution.

3.7. Sizing methodology of system components

A general methodology followed in selecting the size of the main

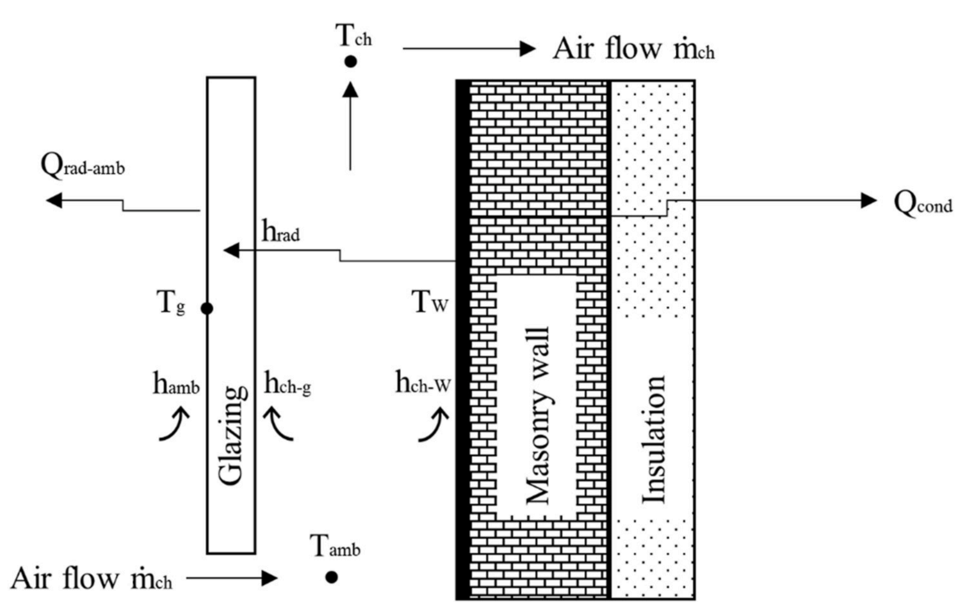

Fig. 3. Schematic of the Trombe wall.

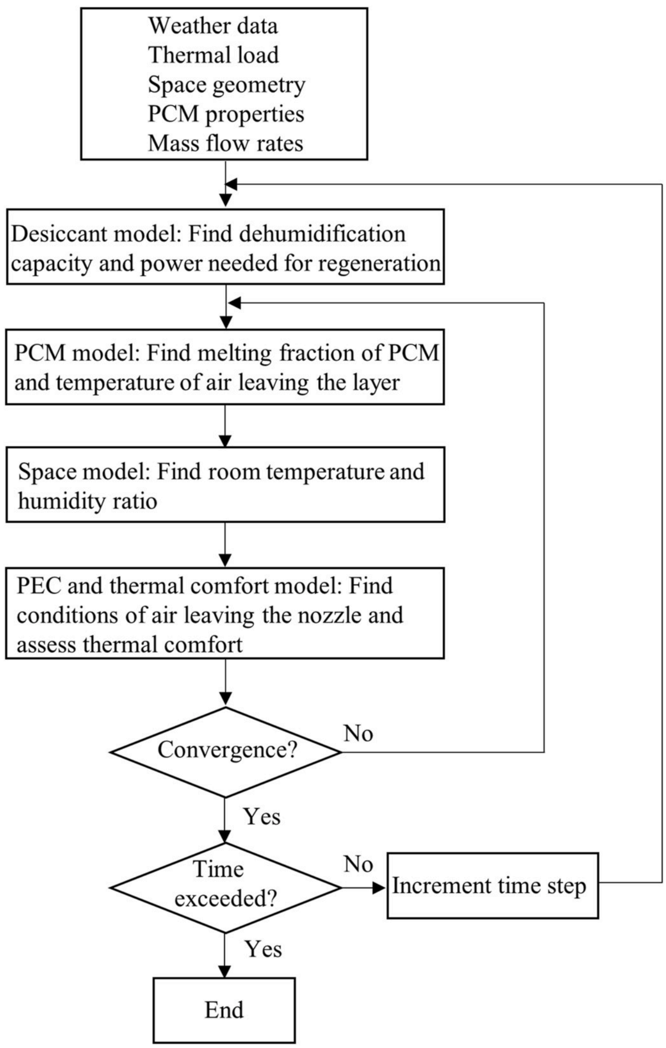

Fig. 4. Flow chart of the proposed system.

system components is presented in this section. The proposed methodology sets the guidelines for utilizing the proposed system and applying it to different encountered case studies in real applications. The data needed to size the different system components are mainly the weather conditions in terms of ambient hourly temperature, humidity and solar radiation, characteristics of the office space (envelop properties and space geometry) and the cooling load over the occupied hours, and number of occupants. The different components are sized according to the data provided as follows:

- The amount of fresh air needed depends on the number of occupants inside the space such that a minimum ventilation rate of 7 l/s per person is maintained as recommended by ASHRAE [33].
- The selection of the PCM melting temperature depends on the peak cooling load and on the lowest diurnal temperature difference with highest humidity levels during the night. The system should be capable of removing the cooling load to maintain a room temperature around 29 °C during occupied hours, and solidifying the PCM using evaporative cooling during the night. The cooling load of the room dictates the upper limit of the PCM temperature as it needs to be low enough (below 29 °C) to remove the load. The nighttime wet bulb temperature dictates the lower limit of the PCM melting temperature so that total PCM solidification is feasible.
- The PCM mass is selected such that the PCM removes the cooling load during the hottest day in the summer months, while completely melting by the end of the occupancy hours. The cooling load is defined as the energy needed to cool the room air to an acceptable temperature of around 29 °C when using a PEC [11]. The PCM layer surface area and air channel length are limited by the space ceiling area (length × width); accordingly, the PCM layer thickness can be found.
- The size of the auxiliary heater depends on both the weather conditions (mainly humidity and solar radiation) and the efficiency of the Trombe wall in heating the outdoor air. For the most critical conditions when the outdoor air has the highest humidity, the required regeneration temperature would be the highest to maintain an acceptable room relative humidity just below the maximum allowable limit of 65% as set by ASHRAE [33]. The auxiliary heater needs to provide the additional energy needed when the Trombe wall fails to attain the desired regeneration temperature.

The proposed sizing methodology was implemented in the following case study that considers an office space occupied during the day over the summer months of Beirut climate.

4. Case study

The current study evaluated the performance of the proposed system in providing indoor thermal comfort. A case study of an office space (7 m × 6 m × 3 m) in Beirut was simulated during the summer months for each typical representative day from June to September. The weather data was obtained using TMY (Typical Meteorological Year) for Beirut using Meteonorm (V7.3) database, as done by many researchers including Chan et al. [44], Farah et al. [45], Annan et al. [46], and Daaboul et al. [47]. The TMY produces typical weather data by using statistics performed over a number of years to present data of the highest occurrence. For Meteonorm, the TMY data is predicted based on a 10-year period extending from 2000 to 2009 with the data for a representative day of each month shown in Table 1. For the energy consumption over the entire summer month, the energy consumed during a typical day of each month is multiplied by the number of days of that month.

The office was occupied during the typical working schedule in Lebanon, from 8:00am to 5:00pm.The occupancy schedule, shown in Fig. 6, was obtained such that the maximum number of occupants at once in the office space was three following ASHRAE's recommendation [33] with a minimum of 14 m^2 of office area per occupant. According to ASHRAE [30], each occupant contributes 75 W sensible load and 55 W latent load to the space load. The lighting and equipment loads were estimated at 84 W per occupant [33].

The main components of the system include the desiccant wheel, the sensible wheel, Trombe wall, PCM storage layer, and the PEC. Table 2 shows the selected dimensions of these components.

The Trombe wall was incorporated into the building envelope at the south wall which was made up of a clear single glazing, an air channel (4 cm thick) as recommended by Kessel [49], a double layered wall composed of a polystyrene insulation layer, and a masonry concrete wall coated with a dark heat absorbing material as used by Badawiyeh et al. [39]. The space was also made up of an external wall on the east side while the remaining space envelope were internal surfaces partitioned with conditioned spaces with their properties obtained from the thermal standards for buildings in Lebanon [50]. The properties of the Trombe wall and the space envelope properties are found in Table 3.

The supply of fresh air was chosen based on the occupancy schedule of the space following ASHRAE standards [33] of minimum required ventilation rate per occupant (7 l/s per person). The flow rate of the air passing through the Trombe wall was set to be equal to the supply flow rate of fresh air as recommended by Beccali et al. [38]. The PEC flow rate was selected based on human thermal comfort standards (7 l/s) [26] and it was constantly maintained throughout the occupancy hours and the simulations for all of the months. The supply flow rate of air to the space

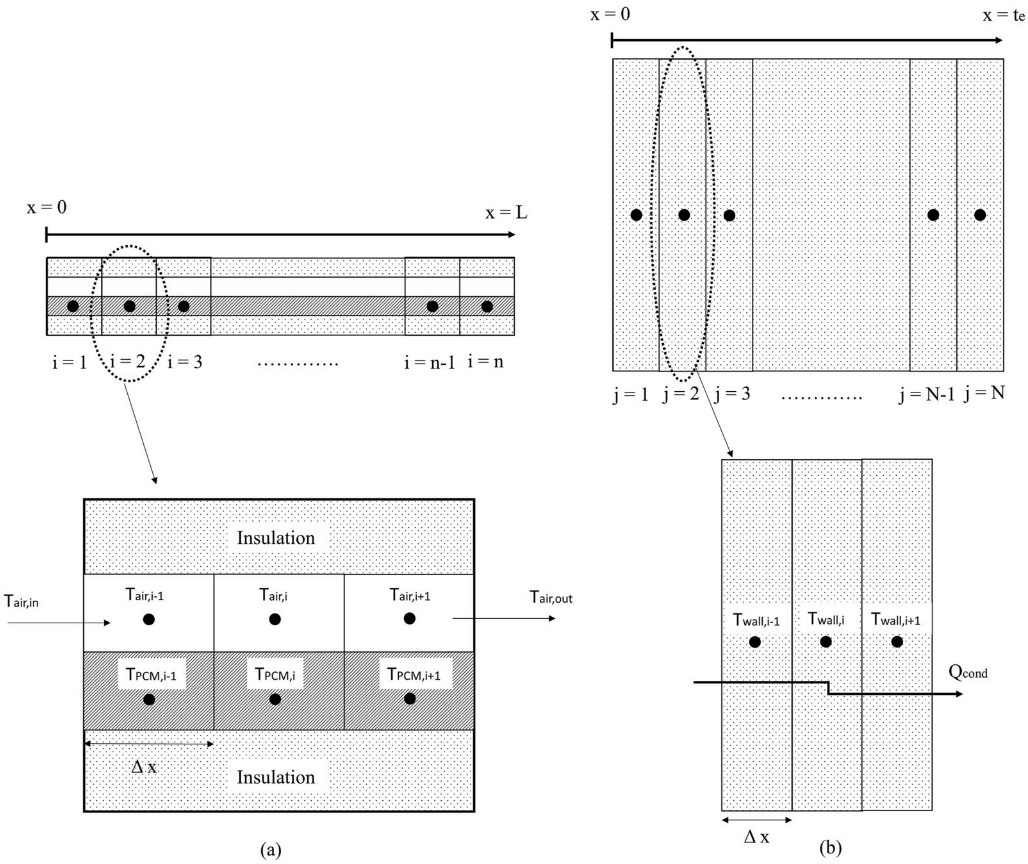

Fig. 5. Discretization of (a) PCM storage layer and (b) envelope element.

Table 1
Ambient conditions for typical days in each summer month.

Time	June			July			August			September		
	T_{amb} (°C)	T_{wb} (°C)	I (W/m^2)	T_{amb} (°C)	T_{wb} (°C)	I (W/m^2)	T_{amb} (°C)	T_{wb} (°C)	I (W/m^2)	T_{amb} (°C)	T_{wb} (°C)	I (W/m^2)
00:00	23	19	0	27	22	0	27	22	0	26	21	0
1:00	23	18	0	27	22	0	27	21	0	26	21	0
2:00	23	18	0	27	21	0	27	21	0	26	20	0
3:00	23	18	0	27	21	0	27	20	0	26	20	0
4:00	23	18	0	26	21	0	27	20	0	25	20	0
5:00	23	18	0	26	21	0	27	20	0	25	20	0
6:00	23	18	14	26	21	3	26	21	0	25	20	0
7:00	23	19	270	26	21	218	27	21	126	25	20	44
8:00	25	19	445	28	22	420	28	22	443	26	21	410
9:00	25	20	525	28	22	511	29	22	577	27	21	585
10:00	26	21	567	29	22	558	29	23	640	28	21	660
11:00	26	21	590	29	23	583	30	23	673	28	22	697
12:00	26	22	602	30	23	596	30	24	690	28	22	715
13:00	27	22	607	30	24	601	30	24	694	29	22	721
14:00	27	23	604	30	24	599	30	25	681	29	22	716
15:00	27	23	594	30	24	590	30	25	655	29	23	700
16:00	27	23	574	30	24	570	30	25	607	29	23	665
17:00	26	23	538	29	24	535	30	25	510	28	23	595
18:00	26	23	471	29	24	468	29	25	285	28	23	436
19:00	26	23	331	28	24	328	29	25	6	28	23	67
20:00	26	22	49	27	24	48	28	25	0	28	23	0
21:00	26	22	0	27	24	0	28	24	0	27	22	0
22:00	25	21	0	27	23	0	28	24	0	27	22	0
23:00	25	20	0	27	23	0	28	23	0	27	21	0

was chosen based on ASHRAE's minimum ventilation rate (92 l/s) [33]. A control strategy was adopted to supply the outdoor air to the space 3 h prior to occupancy to refresh the room air with the cooler and less humid ambient air with a flow rate equal to the supply flow rate during occupied hours (92 l/s). For the other unoccupied hours, a small flow rate of outdoor air was filtrated into the space (2 l/s). The flow of the air used to solidify the PCM during nighttime was 11.5 l/s and was selected as such so that a complete solidification was obtained just before the occupancy schedule at the month that had the peak ambient conditions for temperature and humidity, as discussed in section 3.7. For the Beirut

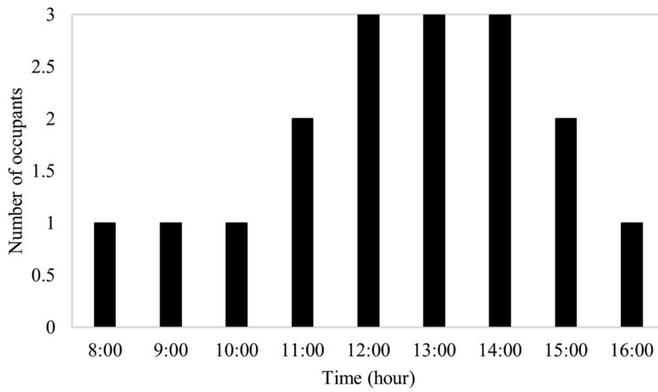

Fig. 6. Occupancy schedule in the space.

Table 2
Dimensions of various components of the integrated system.

Parameter	Properties
Desiccant wheel	Rotor diameter = 482.6 mm; Depth = 345 mm; weight = 67 kg [48]
Sensible wheel	Rotor diameter = 482.6 mm; Depth = 345 mm; weight = 67 kg [48]
Trombe wall	Height = 3 m; width = 6 m; air gap thickness = 4 cm [49]
PCM layer	Length = 6.5 m; width = 5.5 m; thickness = 0.25 mm [17]
PEC	Nozzle diameter = 8 cm; distance away from occupant = 35 cm [35]

Table 3
Space envelope properties.

Parameter	Properties
Glazing	Clear single glazing; $\alpha = 0.06$; $\varepsilon = 0.9$; $\tau = 0.84$
South wall	5 cm polystyrene insulation layer; $k = 0.032$ W/m·K; $\alpha = 0.95$; $\varepsilon = 0.95$; $\rho = 70$ kg/m^3; $C_p = 830$ J/kg·K 25 cm masonry concrete, $k = 1.8$ W/m·K; $\rho = 2800$ Kg/m^3; $C_p = 1200$ J/kg·K
East wall	20 cm concrete Hollow block; $U = 3.03$ W/m^2·K; $\rho = 600$ kg/m^3; $C_p = 1200$ J/kg·K
Internal envelope	10 cm concrete Hollow block; $U = 3.63$ W/m^2·K; $\rho = 600$ kg/m^3; $C_p = 1200$ J/kg·K

climate, it was the month of August.

4.1. PCM selection

The PCM was stored in a thin layer above the insulated ceiling extending to nearly the entire area of the roof. To select the PCM melting temperature and mass, simulations were done for the month with the peak conditions, as discussed in section 3.7. In this case, the highest outdoor air temperature and the most humid weather throughout daytime and nighttime were in August. The PCM melting temperature was selected such that the room macroclimate temperature did not exceed the maximum limit for thermal comfort, which was 29 °C while using a PEC to provide thermal comfort to the occupants [11]. However, to completely solidify the PCM during unoccupied hours and even with the aid of evaporative cooling, the minimum melting PCM temperature was 25 °C. To sustain comfort for the all occupied hours, a minimum of 7.87 kg (5.5 m × 6.5 m with a thickness of 0.25 mm) of PCM should be present. The PCM properties were obtained from Thambidurai et al. [51] and are listed in Table 4.

Table 4
PCM properties.

PCM property	Value
Specific heat	2000 J/kg·K
Density	880 kg/m^3
Latent heat of fusion	210 kJ/kg

4.2. Regeneration temperature selection

The regeneration temperature of a desiccant wheel using Silica gel as the desiccant should be within the range from 40 °C to 80 °C as recommended by Beccali et al. [37]. The regeneration temperature was fixed throughout the day for each month while maintaining a room relative humidity below 65%, as discussed in section 3.7. Simulations were performed for June, July, August, and September with the minimum regeneration temperature to keep the relative humidity of the space just below the maximum allowable limit were found to be 55 °C, 51 °C, 57 °C, and 40 °C, respectively. Whenever the Trombe wall was not enough to obtain the required regeneration temperature, the auxiliary heater provided the desired regeneration throughout the day.

4.3. Conventional system setup

To evaluate the performance of the proposed system, a conventional air conditioning system was simulated to compare the energy consumption of both systems. The conventional air conditioning system is a regular vapor compression system that provides uniform conditions in the space. Accordingly, assessing comfort using the Predicted Mean Vote (*PMV*) [52] and for the same thermal comfort level, the energy consumption of the two systems were compared. Simulations were performed for each month to find the electric energy needed to remove the sensible and latent loads for the same room envelope, supply air flow rate, fresh air flow rate, and ambient conditions used for the proposed system. The energy consumption of the conventional system is composed of the electrical energy consumed to run the mechanical cooling system whereas the proposed system's energy consumption is made up of the electrical energy used to run the fans and the rotors of the desiccant and sensible wheels. In addition, the proposed system consumes low grade thermal energy used by the auxiliary heater to reach the required regeneration temperature.

4.4. System performance indicators and constraints

The performance of the system will be evaluated based on its energy consumption, the thermal comfort it provides for the occupants, and indoor air quality. The performance indicators of these criteria are presented below:

- The energy consumption of the system is composed of the thermal energy needed by the auxiliary heater for regeneration and the electrical energy used by the latent and sensible wheels and the fans.
- The system should maintain occupant thermal comfort above the level of slightly uncomfortable (−1) on Zhang's et al. [36] thermal comfort scale.
- The COP of the proposed system, which is the ratio of the cooling load of the space to the thermal energy consumed through direct heating and electrical energy converted to thermal used by the system to remove the load. The system cooling load is defined in Eq. (13) as the thermal energy removed by the system while cooling the ambient air to the air supplied to the space after leaving the PCM, and the energy removed while cooling the return air circulating within the space.

$$Q_{cooling} = \dot{m}_{fresh}\left(H_{amb} - H_{sup}\right) + \dot{m}_{return} C_p \left(T_{room} - T_{sup}\right) \tag{13}$$

where $Q_{cooling}$ is the cooling load of the space (W), H_{amb} and H_{sup} are the enthalpies of the ambient and supply air, respectively (J/kg), and $\dot{m}_{fresh}$ and $\dot{m}_{return}$are the flow rates of the fresh air and air recirculated within the space, respectively (kg/s).

The energy consumed by the proposed system is made of the auxiliary heater thermal energy and the electrical energy used in the system converted to thermal raw energy for electric power generation. A typical power plant has a thermal-to-electric efficiency of 47% as presented by Zaversky et al. [53]. The peak and daily average COP will be calculated to measure the performance of the system. The peak COP is calculated for the critical hour of the day, when the cooling load is at its peak, and is given by

$$COP_p = \frac{Q_{cooling,p}}{Q_{aux,p} + \frac{Q_{E,p}}{\mu}} \tag{14}$$

where $Q_{cooling,p}$ is the cooling load at the peak hour (W), $Q_{aux,p}$ and $Q_{E,p}$ are the thermal and electric energy consumed by the system at the peak hour, respectively (W), and μ is the thermal-to-electric efficiency (%).

The daily average COP is found by calculating the cooling load and energy consumption over the entire day and is given by

$$COP_{da} = \frac{Q_{cooling,T}}{Q_{aux,T} + \frac{Q_{E,T}}{\mu}} \tag{15}$$

where $Q_{cooling,T}$ is the total cooling load over the entire day (W) and $Q_{aux,T}$ and $Q_{E,T}$ are the total thermal and electric energy consumed by the system over the entire day, respectively (W).

The constraints on the performance of the system are as follows:

- The maximum room relative humidity is 65% as recommended by ASHRAE [33].
- The minimum supply of fresh air is 7 l/s per occupant as recommended by ASHRAE [33].
- The PCM should completely solidify during unoccupied hours to maintain the system performance for the next day.

5. Results and discussion

The proposed system is assessed based on the simulations of the developed mathematical model, the level of the indoor thermal comfort, and the energy consumption for each summer month. The effectiveness of the Trombe wall in reducing energy consumption was determined by comparing the energy consumption of the system with and without it. Finally, the system performance was evaluated by finding the energy savings the system can yield compared with a conventional AC unit. The system was simulated for a typical day for each summer month (June, July, August, and September) with August being the most critical month.

5.1. Model validation

The accuracy of the obtained results depends on the accuracy of the desiccant model, Trombe wall, PCM model, and space model. These models are experimentally validated with a small relative error in measurement. The desiccant wheel model developed by Beccali et al. [37] was derived from the interpolation of experimental data. The theoretical Trombe wall model developed by Ong et al. [40] was verified by conducting an experiment with a physical model of a Trombe wall (2 m high × 0.45 m wide) with air gaps of 0.1, 0.2, and 0.3 m under varying ambient conditions. The experiments were carried out outdoors and on the roof of the building such that the setup was exposed to both direct and diffuse solar radiation. The PCM model presented by Lin et al. [17] was validated using the data collected from a laboratory experimental air-conditioning test rig. During the tests, a total of five PCM bricks were placed at the end of the air duct as a test section. The PCM melting temperature used was 23 °C with each PCM brick having the dimensions of 0.5 m × 0.25 m × 0.032 m while the air layer was 16 mm thick. As for the space model presented by Yassine et al. [34], it was validated against a calibrated software (TRNSYS). Table 5 shows the relative error of each model discussed in the literature, which developed and validated the model. It is observed that the overall operation has a small error of measurement making the obtained results reliable.

5.2. Analysis of indoor conditions and thermal comfort

Fig. 7 to Fig. 10 present the variation in time of (a) the temperature of the room and ambient air while showing the temperature range of the PEC outlet and the overall comfort levels during occupied hours, and (b) the humidity ratio of room and ambient air for the months of June, July, August and September, respectively. To maintain comfort within the space, the maximum allowable room temperature is 29 °C when using a PEC [26]. As for the humidity, the maximum allowable relative humidity inside the space is 65% as set by ASHRAE [33]. The desiccant wheel, Trombe wall, and PEC were turned on during the occupied hours and turned off during the unoccupied. The flow rate of air passing through the desiccant wheel and the Trombe wall varied per the occupancy schedule while the PEC flow rate was maintained throughout the occupancy hours.

For the month of June (Fig. 7), the room temperature varied between 24.8 °C and 26.3 °C during occupancy hours (see Fig. 7 (a)) which is below the maximum allowable room temperature of 29 °C. The room temperature increased steadily as the occupancy hours began and decreased slightly towards the end of the occupancy schedule. This was due to the change of the occupancy schedule and thus resulted in a decrease in the internal load. During unoccupied hours, the room temperature slightly decreased with the decrease of the ambient through exchanging heat with the walls and a small flow rate of ambient air due to infiltration. Before 3 h of the occupancy schedule, the supply fan was turned on to refresh the ambient air, which is cooler and less humid than the room air, hence providing a noticeable decrease in the temperature and humidity of the room air. The PEC outlet temperature varied slightly between 19.4 °C and 21.5 °C (see Fig. 7 (a)). The overall thermal comfort of the occupants was found using Zhang's thermal comfort model [36] between −0.34 and + 0.32 and which fell above the limit of the minimum acceptable thermal comfort of −1 or slightly uncomfortable. Even though the PEC increased the moisture generation in the space, desiccant dehumidification maintained the room relative humidity between 58% and 63% both below the maximum allowable limit of 65%.

5.3. Hybrid system component evaluation

To prove the contribution of each subsystem in the overall system operation, Table 6 shows the temperature and humidity ratio of the air leaving each component as labeled in Fig. 1 during daytime operation at the peak occupancy hour (3:00 p.m.). In June for example, the ambient humidity ratio at state 1 entering the desiccant wheel at 15.6 g/kg is dehumidified and leaves the desiccant at state 2 with a lower humidity ratio of 10.0 g/kg while increasing its temperature from 27 °C to 43.6 °C. Evaporative cooling is used to cool the dehumidified air through exchanging heat between the evaporatively cooled ambient air and the dehumidified air using a sensible wheel. The dehumidified air leaving the sensible wheel at state 3 with a temperature of 26.4 °C mixes with the room return air to reach state 4. The mixed air is cooled while

Table 5
Reported relative error of measurement of each model.

Model	Error in temperature (°C)	Error in humidity ratio (g/kg)
Desiccant model	±0.15 [37]	±0.20 [37]
Trombe wall model	±0.50 [40]	–
PCM model	±0.30 [17]	–
Space model	±0.40 [34]	–

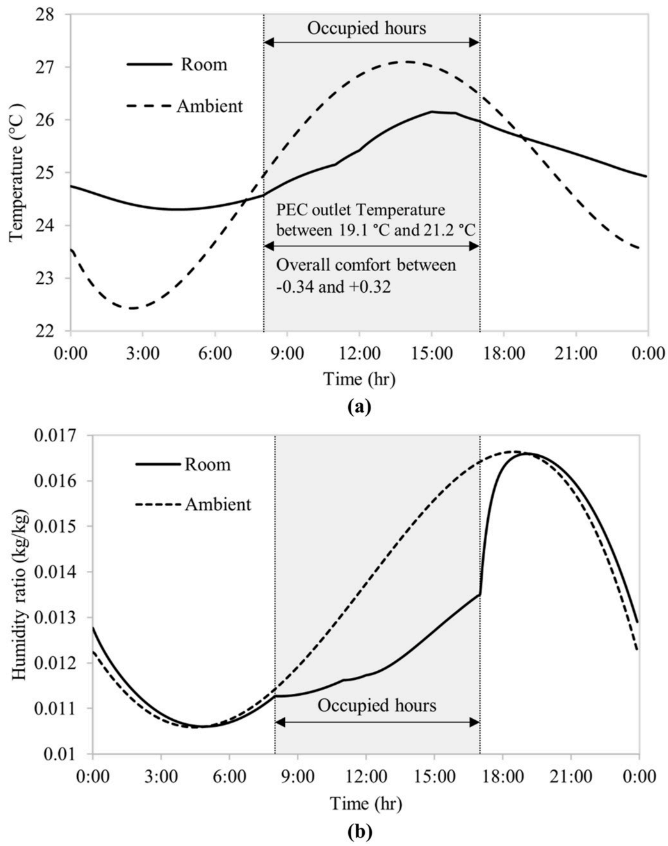

Fig. 7. The variation in time of (a) the temperature of the room and ambient air while showing the temperature range of the PEC outlet and the overall comfort levels during occupied hours and (b) the humidity ratio of room and ambient air for the month of June.

Table 6
Temperature and humidity ratio at each state of the system for each month at the peak occupancy hour (3:00 p.m.).

Month	June		July		August		September	
State	*T* (°C)	*w* (g/kg)	*T* (°C)	*w* (g/kg)	*T* (°C)	*w* (g/kg)	*T* (°C)	*w* (g/kg)
1	27.0	15.6	30.0	16.2	30.0	17.4	28.9	14.4
2	43.6	10.0	43.3	11.7	46.7	11.8	38.4	11.0
3	26.4	10.0	27.5	11.7	28.7	11.8	25.8	11.0
4	26.3	12.1	28.0	13.8	28.3	13.9	26.9	13.3
5	26.1	12.1	27.5	13.8	27.7	13.9	26.5	13.3
6	21.0	14.8	22.9	16.6	23.0	16.7	22.3	16.0
7	26.3	12.7	28.2	14.4	28.2	14.6	27.2	14.0
A	27.0	15.6	30.0	16.2	30.0	17.4	28.9	14.4
B	38.5	15.6	41.2	16.2	43.0	17.4	44.0	14.4
C	55.0	15.6	51.0	16.2	57.0	17.4	44.0	14.4

1: Outdoor air; 2: Exit of desiccant wheel; 3: Exit of sensible wheel; 4: Mixed air after sensible wheel and return room air; 5: Exit of PCM layer; 6: Exit of PEC; 7: Return room air; A: Outdoor air; B: Exit of Trombe wall; C: Exit of Auxiliary heater.

passing through the PCM layer from 26.3 °C to 26.1 °C before being supplied to the space. The supplied air at state 5 (temperature 26.1 °C and 12.1 g/kg humidity ratio) enters the room and enters the PEC which cools the air delivered to the upper body segments of the occupants to 21 °C while humidifying the air to 14.1 g/kg. Finally, part of the room air at state 7 (26.3 °C and 12.7 g/kg) is exhausted to the ambient while the other part is recirculated in the space. On the regeneration stream, the ambient air at state A at temperature of 27 °C is heated after passing through the Trombe wall and leaves with an elevated temperature of 38.5 °C. To reach the desired temperature of 55 °C, the auxiliary heater is used to heat the air leaving the Trombe wall at state B to reach state C.

As for the months of July, August, and September (Fig. 8 to Fig. 10) they had similar weather conditions with August being the hottest and most humid month. The room temperature remained below the maximum allowable macroclimate temperature of 29 °C where it reached a maximum of 28.2 °C in August (see Fig. 9(a)). In addition, with the aid of the desiccant wheel the room relative humidity remained below 65% during the occupied hours while varying the minimum regeneration temperature for each month. The overall comfort of the occupants was also just at the limit of the minimum thermal comfort level while obtaining slightly better results for July and September, which have a drier cooler climate than August. The conditions of the air leaving each component of the proposed system for the months of July, August, and September are also shown in Table 6. The components operate in a similar manner for all the months while the conditions of the air vary due to the variation in the ambient conditions and required regeneration temperature.

For September, the humidity ratio of the room has a different trend than the other months (see Fig. 10(b)) where the room humidity ratio is higher than the ambient in the first hours of occupancy. This occurs due to the relatively low ambient humidity and high temperature such that even with the moisture generation from the PEC and occupants in the space, the room relative humidity remains below 65% and so comfort is attained. As for the remaining occupancy hours towards the end of the day, the ambient humidity was high and the moisture generation increased with the increase of the number of occupants as per the occupancy schedule. Hence, dehumidification was required to maintain the thermal comfort limit for the maximum allowable humidity in the space. In addition, the Trombe wall provided extra regeneration above

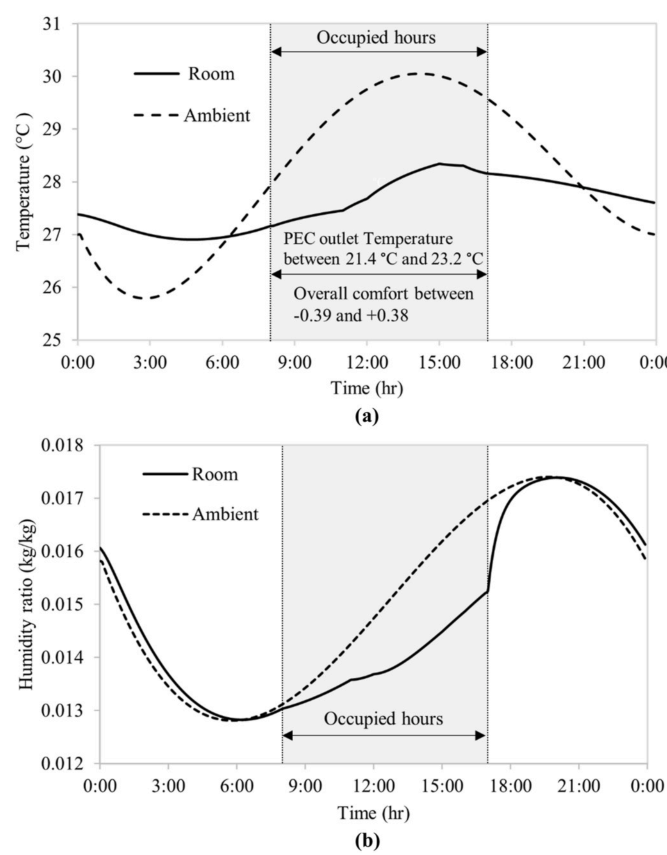

Fig. 8. The variation in time of (a) the temperature of the room and ambient air while showing the temperature range of the PEC outlet and the overall comfort levels during occupied hours and (b) the humidity ratio of room and ambient air for the month of July.

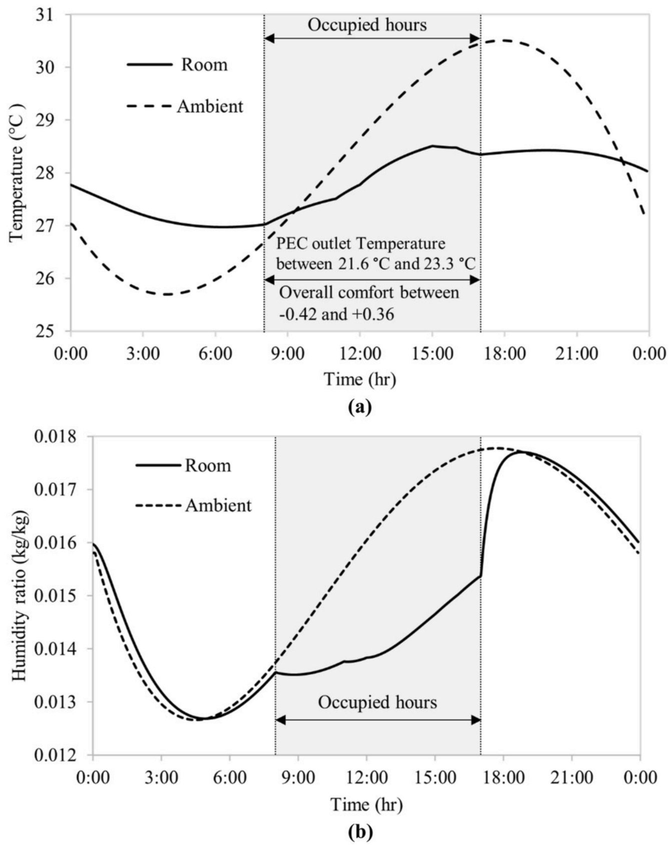

Fig. 9. The variation in time of (a) the temperature of the room and ambient air while showing the temperature range of the PEC outlet and the overall comfort levels during occupied hours and (b) the humidity ratio of room and ambient air for the month of August.

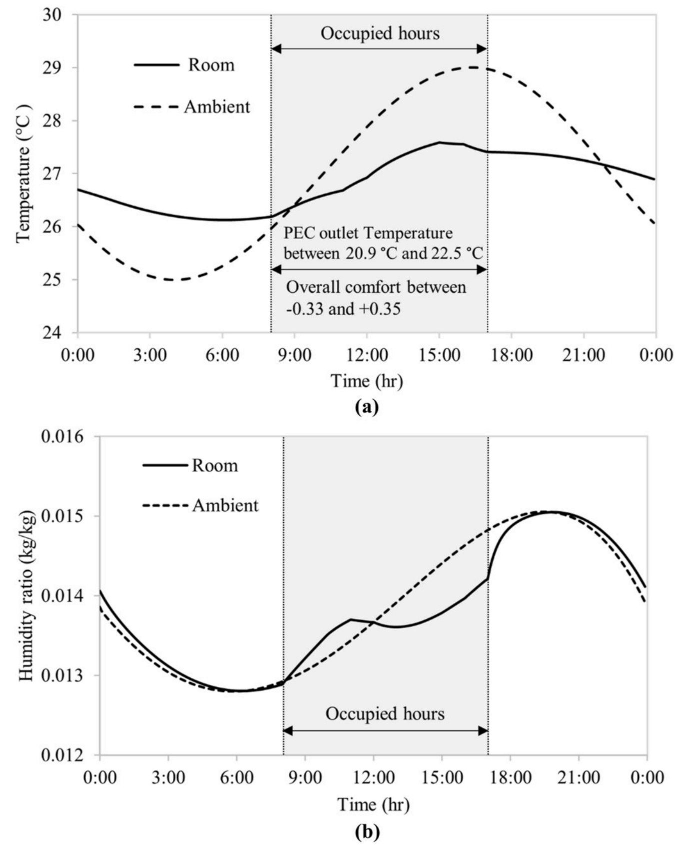

Fig. 10. The variation in time of (a) the temperature of the room and ambient air while showing the temperature range of the PEC outlet and the overall comfort levels during occupied hours and (b) the humidity ratio of room and ambient air for the month of September.

the minimum required limit. Therefore, the relative humidity in the space during the last hours of occupancy was in the range between 58% and 62%, which fell well below the maximum allowable limit of 65%.

As for the PCM, it completely solidified during the night in all months with the aid of evaporative cooling of the ambient air except for the month of June, where the ambient air was cool enough for PCM solidification and so the evaporative cooler was unnecessary. The flow rate of the air used for the solidification process was the minimum flow rate to obtain complete solidification just before the occupancy hours begin for the most critical month (August). The PCM completely melted only in August and at the end of the occupied hours lasting the whole duration of the occupancy (9 h). Solidification occurred faster in the months other than August as the PCM did not completely melt. In June, only 26% of the PCM melted requiring only 3.1 h to completely solidify compared to 8.3 h in August.

If the heat from the Trombe wall was not enough to heat the air to the minimum needed regeneration temperature for each month, the auxiliary heater was used. Table 7 presents the hourly energy consumption of the auxiliary heater (Q_{aux}) and the temperature of the air leaving the Trombe wall channel (T_{ch}). The temperature of the air leaving the Trombe wall varied hourly due to the time-variation of the solar irradiance and ambient temperature. The energy consumption of the auxiliary heater also varied hourly as per the occupancy schedule since more energy was needed to heat a larger flow of air. The consumption of the heater depended on the variation of the temperature of the air leaving the Trombe wall channel. It was observed that for the month of September, which had the highest solar irradiance compared to the other months, the Trombe wall alone was just enough to obtain a room relative humidity below the maximum limit of 65%. However, in June, which had the lowest solar irradiance and had a relatively high humidity, the total auxiliary heater consumption was found to be the highest among the different months.

To find the energy needed for regenerating the desiccant wheel, the heat energy needed to heat the ambient air to the required minimum regeneration temperature was calculated. The auxiliary heater energy consumption and the Trombe wall energy savings are shown in Fig. 11. The Trombe wall significantly reduced the thermal energy consumption especially in September since it had the highest solar irradiance on the south wall. In September, the auxiliary heater consumed only 1.9 kWh, which was nearly 36 times less than the consumption of the system that relied only on the auxiliary heater for regeneration. Over the entire summer period, the Trombe wall reduced the total thermal energy consumption by 55% compared to using the auxiliary heater solely for regeneration.

The peak and the daily average COP of the proposed system were calculated for the months of August (minimum COP) and September (maximum COP). The peak COP calculated for the critical hour of the day (around 3:00 p.m.) is in the range of 2.4–5.7 and the daily average COP is in the range of 2.9–7.0 (lower limit is the COP for the month of August and upper limit for September).

If the regeneration energy depended solely on auxiliary heating, the peak COP would be in the range of 1.4–2.3 and the daily average COP would be in the range of 1.8–2.6. It is perceived that there is a significant difference between the COP of the system with and without using a Trombe wall for regeneration, which signifies the degree of the energy savings while implementing a Trombe wall in this system.

5.4. Energy performance comparison with conventional cooling system

The performance of the proposed cooling system was evaluated by

Table 7
Temperature of the air leaving the Trombe wall and the needed auxiliary heater power for regeneration during each month.

Month	June (T_{reg} = 55 °C)			July (T_{reg} = 51 °C)			August (T_{reg} = 57 °C)			Sep (T_{reg} = 40 °C)		
Time	T_{amb} (°C)	T_{ch} (°C)	Q_{aux} (W)	T_{amb} (°C)	T_{ch} (°C)	Q_{aux} (W)	T_{amb} (°C)	T_{ch} (°C)	Q_{aux} (W)	T_{amb} (°C)	T_{ch} (°C)	Q_{aux} (W)
8:00–9:00	25	34	176	28	37	122	28	35	187	26	34	55
9:00–10:00	25	37	151	28	40	97	29	40	147	27	39	10
10:00–11:00	26	38	142	29	41	85	29	42	130	28	42	0
11:00–12:00	26	38	273	29	41	164	30	42	245	28	43	0
12:00–13:00	26	38	420	30	41	253	30	42	383	28	43	0
13:00–14:00	27	38	425	30	41	255	30	42	382	29	43	0
14:00–15:00	27	38	423	30	41	252	30	43	365	29	44	0
15:00–16:00	27	39	284	30	42	160	30	44	232	29	45	0
16:00–17:00	27	40	138	30	43	73	30	46	107	29	47	0

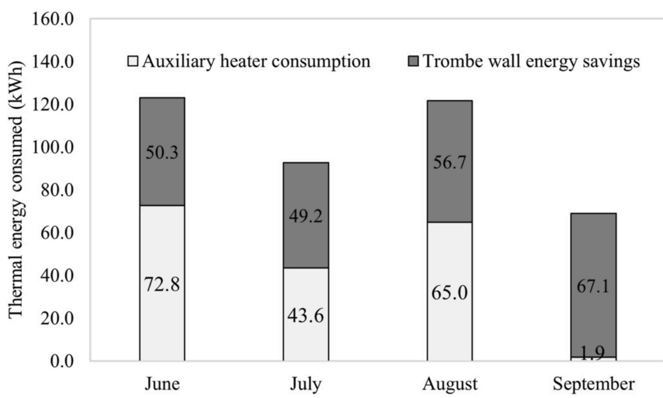

Fig. 11. Thermal energy consumption of the auxiliary heater of the proposed system and the energy savings of the Trombe wall.

comparing its consumption with the consumption of a mechanical ventilation system that utilizes a direct expansion system with a typical coefficient of performance of 3.0 [39] to obtain the same comfort level. The average thermal comfort obtained using the proposed system on Zhang et al. [36] scale is −0.010, −0.005, −0.030, 0.010 for June, July, August, and September, respectively, which correspond to a nearly neutral state on the *PMV* scale. Simulations were performed for each month to find the electric energy needed to remove the sensible and latent loads for the same room envelope, supply air flow rate, fresh air flow rate, and ambient conditions used for the proposed system.

As for the electric consumption of the proposed system, it was made up of the consumption of the fans of the supply air, fresh air, air used to solidify the PCM, air passing through the Trombe wall, air passing through the sensible wheel, and the PEC, as well as, the power to rotate the desiccant wheel. Comparing the performance of the proposed system with a conventional AC unit, Table 8 presents the electrical energy consumption of both the proposed system and the conventional one. The results showed significant electrical savings especially in August where the electrical energy saving was 159.4 kWh which amounted to 96% energy reduction. The overall electrical energy saving for the entire summer period was 513.5 kWh corresponding to nearly 95% of the electric consumption of the conventional AC system.

The energy consumed by the conventional AC unit was compared to the consumption of the proposed system such that thermal comfort is maintained by both systems. If the conventional AC system were to provide a uniform space temperature profile similar to the profile obtained by the proposed system while maintaining a room relative humidity below the maximum allowable limit, the energy consumption of the conventional AC would be different. For a room set-point temperature between 27 °C and 28 °C and a relative humidity below 65%, the conventional AC unit would consume 51 kWh to maintain the space conditions for the critical month of August. The same room conditions were maintained while using the proposed system consuming only 6.3 kWh.

The cost of operation of each system per month was calculated and the results are shown in Fig. 12. The calculations were based on a pricing of 5 cents/kWh of central heating and 20 cents/kWh of electrical energy. The proposed system achieved significant savings especially in the month of September where the conventional system cost $23.7, which was nearly 18 times more than the proposed system. Even in the month of June, the savings remained substantial as the system saved up to 75% compared with the conventional AC system. Overall, the proposed hybrid cooling system achieved savings amounting to 87% over the entire summer period from the conventional AC system.

Table 8
Electrical energy consumed by a conventional AC unit compared with the proposed system during the entire month.

Electrical consumption (kWh)	Conventional AC unit	Proposed system
June	95.6	6.0
July	158.3	6.2
August	165.7	6.3
September	118.5	6.1

5.5. *Limitations and applicability*

The proposed hybrid cooling system is feasible in hot and humid climates; however, there are some limitations like the case with other hybrid systems. The system in the current design cannot be implemented in residential buildings as nighttime operation is dedicated for the solidification of the PCM. In addition, solar energy is not available during nighttime so a large amount of auxiliary heating would be needed to dehumidify the air at night in humid climates. Furthermore, this system cannot provide thermal comfort if there are higher internal loads for the same space parameters. The system can only provide comfort for typical low occupancy office spaces (load does not exceed 80 W/m^2).

The applicability of the proposed system has been shown in the case

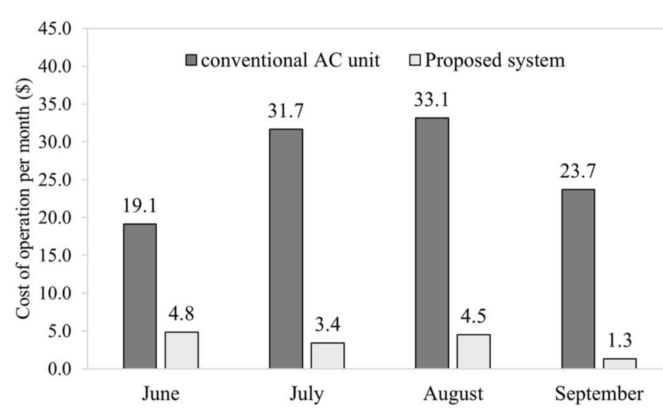

Fig. 12. The cost of operating a conventional AC unit and the proposed system for each month.

study for hot and humid conditions. The sizing and selection approach as well as the performance indicators of the various system components were presented. On the other hand, the proposed system can be applied in different climates of dryer and relatively cooler conditions. Lower humidity levels would reduce the need for auxiliary heating and might eliminate the need for a Trombe wall and desiccant dehumidification. Moreover, a lower PCM melting temperature could be selected if nighttime conditions are dryer with lower wet bulb temperatures, thus the system would be more efficient in removing higher cooling loads during the day. Moving forward, even though this system is typically applied to a single office space it can also be implemented on a much larger scale such as an entire office building, which can yield more energy savings and make the system more economically feasible. In addition, applying another heating source simultaneously with the Trombe wall instead of the auxiliary heater such as solar energy or a waste heat source could vastly improve the performance of the system and increase energy savings.

6. Conclusions

This paper investigated the feasibility of implementing a hybrid cooling system for an office space in a hot and humid climate. The proposed system was numerically simulated using experimentally validated models with the following key results:

- The thermal comfort of the occupants was maintained between a neutral and slightly uncomfortable state.
- The room relative humidity was controlled such that it did not exceed the maximum allowable limit.
- Complete solidification of the PCM was achieved during unoccupied hours even for the most critical summer month (August).

As for the energy savings, the proposed system was found to reduce energy cost by 87% compared with a conventional cooling system over the entire cooling season. The Trombe wall savings were also evaluated and it was found that the Trombe wall could save up to 55% of the thermal energy consumption of the proposed system over the entire summer period compared with the case of relying only on the auxiliary heater for regeneration.

Declaration of competing interest

The authors declare that they have no known competing financial interests or personal relationships that could have appeared to influence the work reported in this paper.

CRediT authorship contribution statement

Mohamad El Loubani: Software, Validation. **Nesreen Ghaddar:** Conceptualization, Supervision, Project administration. **Kamel Ghali:** Conceptualization, Methodology, Writing - review & editing. **Mariam Itani:** Formal analysis, Writing - review & editing.

Acknowledgment

The authors would like to acknowledge the financial support of the American University of Beirut – University Research Board – Grant award no. 103780.

References

[1] R. Zeinelabdein, S. Omer, G. Gan, Critical review of latent heat storage systems for free cooling in buildings, Renew. Sustain. Energy Rev. 82 (2018) 2843–2868.
[2] L. Yang, Y. Haiyan, J.C. Lam, Thermal comfort and building energy consumption implications – a review, Appl. Energy 115 (2014) 164–173.
[3] E. Cuce, D. Harjunowibowo, P.M. Cuce, Renewable and sustainable energy saving strategies for greenhouse systems: a comprehensive review, Renew. Sustain. Energy Rev. 64 (2016) 34–59.
[4] R. Zeinelabdein, O.S., E. Mohamed, I. Amaireh, G. Gan, Free cooling based change material for domestic buildings in hot arid climate, in: 16th International Conference on Sustainable Energy Technologies, 2017. Bologna, Italy.
[5] D. Lefebvre, H.F. Tezel, A review of energy storage technologies with a focus on adsorption thermal energy storage processes for heating applications, Renew. Sustain. Energy Rev. 67 (2017) 116–125.
[6] M. Dardir, K. Panchabikesan, F. Haghighat, M. El Mankibi, Y. Yuan, Opportunities and challenges of PCM-to-air heat exchangers (PAHXs) for building free cooling applications—a comprehensive review, J. Energy Storage 22 (2019) 157–175.
[7] A. Waqas, Z. Ud Din, Phase change material (PCM) storage for free cooling of buildings—a review, Renew. Sustain. Energy Rev. 18 (2013) 607–625.
[8] M. Anisura, M. Mahfuza, M. Kibriaa, R. Saidura, I. Metselaara, T. Mahlia, Curbing global warming with phase change materials for energy storage, Renew. Sustain. Energy Rev. 18 (2013) 23–30.
[9] P. Tatsidjodoun, N. Le Pierrès, L. Luo, A review of potential materials for thermal energy storage in building applications, Renew. Sustain. Energy Rev. 18 (2013) 327–349.
[10] D. Fernandes, F. Pitié, G. Cáceres, J. Baeyens, Thermal energy storage: "How previous findings determine current research priorities", Energy 39 (2012) 246–257.
[11] H. Zhang, Human Thermal Sensation and Comfort in Transient and Non-uniform Thermal Environments, PhD thesis, University of California, Berkeley, 2003.
[12] Y. Zhang, R. Zhao, Effect of local exposure on human responses, Build. Environ. 42 (2007) 2737–2745.
[13] F. Souayfane, F. Fardoun, P.-H. Biwole, Phase change materials (PCM) for cooling applications in buildings: a review, Energy Build. 129 (2016) 396–431.
[14] Y. Zhou, S. Zheng, G. Zhang, Study on the energy performance enhancement of a new PCMs integrated hybrid system with the active cooling and hybrid ventilations, Energy 179 (2019) 111–128.
[15] E. Katramiz, N. Ghaddar, K. Ghali, Daytime radiative cooling: to what extent it enhances office cooling system performance in comparison to night cooling in semi-arid climate? J. Build. Eng. 28 (2020), 101020.
[16] A. Heidari, R. Roshandel, V. Vakiloroaya, An innovative solar assisted desiccant-based evaporative cooling system for co-production of water and cooling in hot and humid climate, Energy Convers. Manag. 185 (2019) 396–409.
[17] W. Lin, Z. Ma, M.I. Sohel, P. Cooper, Development and evaluation of a ceiling ventilation system enhanced by solar photovoltaic thermal collectors and phase change materials, Energy Convers. Manag. 88 (2014) 218–230.
[18] Y. Zhou, S. Zheng, G. Zhang, Multivariable optimisation of a new PCMs integrated hybrid renewable system with active cooling and hybrid ventilations, J. Build. Eng. 26 (2019), 100845.
[19] Y. Zhou, S. Zheng, G. Zhang, A review on cooling performance enhancement for phase change materials integrated systems—flexible design and smart control with machine learning applications, Build. Environ. 174 (2020), 106786.
[20] M. Itani, R. Bachnak, N. Ghaddar, K. Ghali, Evaluating performance of hybrid PCM-fan and hybrid PCM-desiccant vests in moderate and hot climates, J. Build. Eng. 22 (2019) 383–396.
[21] E. Osterman, V. Butala, U. Stritih, PCM thermal storage system for 'free' heating and cooling of buildings, Energy Build. 106 (2015) 125–133.
[22] G. Knudsen, A. Melikov, Human response to individually controlled environment, in: Proceedings: Indoor Air, Lyngby, Denmark, 2005.
[23] R. Cermak, A. Melikov, L. Forejt, O. Kovar, Performance of personalized ventilation in conjunction with mixing and displacement ventilation, HVAC R Res. 12 (2006) 295–311.
[24] S. Sekhar, N. Gong, K. Tham, K. Cheong, A. Melikov, D. Wyon, P. Fanger, Findings of personalized ventilation studies in a hot and humid climate, HVAC R Res. 11 (2005) 603–620.
[25] J. Kaczmarczyk, A. Melikov, P. Fanger, Human response to personalized ventilation and mixing ventilation, Indoor Air 14 (2004) 18–29.
[26] W. Chakroun, N. Ghaddar, K. Ghali, Chilled ceiling and displacement ventilation aided with personalized evaporative cooler, Energy Build. 43 (2011) 3250–3257.
[27] S. Yamaguchi, K. Saito, Numerical and experimental performance analysis of rotary desiccant wheels, Int. J. Heat Mass Tran. 60 (2013) 51–60.
[28] R. Seblany, N. Ghaddar, K. Ghali, N. Ismail, M. Simonetti, J. Virgone, A. Zoughaib, Humidity control of liquid desiccant membrane ceiling and displacement ventilation system, Appl. Therm. Eng. 144 (2018) 1–12.
[29] S. Misha, S. Mat, M. Ruslan, K. Sopian, Review of solid/liquid desiccant in the drying applications and its regeneration methods, Renew. Sustain. Energy Rev. 16 (2012) 4686–4707.
[30] K. Rambhad, P. Walke, Regeneration of composite desiccant dehumidifier by parabolic trough solar collector: an experimental investigation, Mater. Today: Proceedings 5 (2018) 24358–24366.
[31] D. Jani, M. Mishra, P. Sahoo, Performance analysis of a solid desiccant assisted hybrid space coolingsystem using TRNSYS, J. Build. Eng. 19 (2018) 26–35.
[32] L. Mei, D. Infield, U. Eicker, L. Dennis, V. Fux, Cooling potential of ventilated PV façade and solar air heaters combined with a desiccant cooling machine, Renew. Energy 31 (2006) 1265–1278.
[33] ASHRAE, Thermal Environmental Conditions for Human Occupancy, 2013.
[34] B. Yassine, K. Ghali, N. Ghaddar, I. Srour, G. Chehab, A numerical modeling approach to evaluate energy-efficient mechanical ventilation strategies, Energy Build. 55 (2012) 613–618.

[35] M. Hourani, K. Ghali, N. Ghaddar, Effective desiccant dehumidification system with two-stage evaporative cooling for hot and humid climates, Energy Build. 68 (2014) 329–338.
[36] H. Zhang, E. Arens, C. Huizenga, T. Han, Thermal sensation and comfort models for non-uniform and transient environments, part II: local comfort of individual body parts, Build. Environ. 45 (2010) 389–398.
[37] M. Beccali, F. Butera, R.A.R.S. Guanella, Simplified models for the performance evaluation of desiccant wheel dehumidification, Int. J. Energy Res. 27 (2003) 17–29.
[38] M. Beccali, R.S. Adhikari, F. Butera, V. Franzitta, Update on desiccant wheel model, Int. J. Energy Res. 28 (2004) 1043–1049.
[39] M. Badawiyeh, N. Ghaddar, K. Ghali, Case study of Trombe wall inducing natural ventilation through cooled basement air to meet space cooling needs, J. Energy Eng. 143 (2) (2017), 04016039.
[40] K. Ong, C. Chow, Performance of a solar chimney, Sol. Energy 74 (2003) 1–17.
[41] M. El-Refaie, S. Kaseb, Speculation in the feasibility of evaporative cooling, Build. Environ. 44 (2009) 826–838.
[42] M. Salloum, N. Ghaddar, K. Ghali, A new transient bioheat model of the human body and its integration to clothing models, Int. J. Therm. Sci. 46 (2007) 371–384.
[43] S. Rajput Kulkarni, Comparative performance of evaporative cooling pads of alternative materials, Int. J. Adv. Sci. Technol. 10 (2011) 239–244.
[44] A. Chan, Developing a modified typical meteorological year weather file for Hong Kong taking into account the urban heat island effect, Build. Environ. 46 (2011) 2434–2441.
[45] S. Farah, W. Saman, J. Boland, Development of robust meteorological year weather data, Renew. Energy 118 (2018) 343–350.
[46] G. Annan, N. Ghaddar, K. Ghali, Natural ventilation in Beirut residential buildings for extended comfort hours, Int. J. Sustain. Energy 35 (2016) 996–1013.
[47] J. Daaboul, K. Ghali, N. Ghaddar, Mixed-mode ventilation and air conditioning as alternative for energy savings: a case study in Beirut current and future climate, Energy Eff. 11 (2017) 13–30.
[48] D. R. I. (Dri), "EcoFresh total recovery wheel," Desiccant Rotors International (DRI).
[49] R. Kessel, Concrete and Concrete Masonry, Cement & Concrete Association of New Zealand, New Zealand, 2017.
[50] Republic of Lebanon Ministry of Public Works and Transport. Energy Analysis and Economic Feasibility, UNDP/GEF, MPWT/DGU, 2005, p. 63.
[51] M. Thambidurai, K. Panchabikesan, K. Mohan, V. Ramalingam, Review on phase change material based free cooling for buildings - the way toward sustainability, J. Energy Storage 4 (2015) 74–88.
[52] P. Fanger, Assessment of man's thermal comfort in practice, Occup. Environ. Med. 30 (1973) 313–324.
[53] F. Zaversky, I. Les, P. Sorbet, M. Sanchez, B. Valentin, J. Brau, F. Siros, The challenge of solar powered combined cycles e Providing dispatchability and increasing efficiency by integrating the open volumetric air receiver technology, Energy 194 (2020) 116796.